JOURNAL OF APPLIED ELECTROCHEMISTRY 12 (1982) 193–204

*Electrocatalytic activation of ruthenium electrodes for the Cl_2 and O_2 evolution reactions by anodic/cathodic cycling**

M. VUKOVIĆ,† H. ANGERSTEIN-KOZLOWSKA, B. E. CONWAY

Chemistry Department, University of Ottawa, Ottawa, Canada

Received 27 May 1981

Ruthenium electrodes subjected to an anodic/cathodic potential cycling regime from 0.06 to 1.4 V E_H develop a changed state of surface oxidation in comparison with that observed in the initial sequence of potentiodynamic sweeps. The cycling effect is analogous to that known at iridium electrodes but here refers to monolayers. The kinetics of Cl_2 and O_2 evolution of these two types of oxidized surfaces were studied by steady-state polarization experiments. Current densities for Cl_2 evolution at the cycled Ru surface oxide are *ca* 30 times greater than those at the original oxidized Ru surface. Oxygen evolution current densities are increased by *ca* 8 times. The effect is a true electrocatalytic one since the real area of the Ru surfaces remains constant within *ca* 5%. The mechanisms of Cl_2 or O_2 evolution appear to remain unchanged, so the electrocatalytic effects observed are tentatively attributed to a change of potential range over which Ru(III) and Ru(IV) oxidation states arise in the oxide film causing modification of electron transfer rates or adsorption of ions and intermediates.

1. Introduction

Interest in the electrochemical properties of ruthenium and ruthenium dioxide electrodes has arisen in the last decade owing to their good electrocatalytic properties for Cl_2 and O_2 evolution reactions and to their stability with regard to corrosion in strong Cl^- ion solutions. Thus 'dimensionanlly stable anodes' (DSA), based on RuO_2 on a titanium substrate, have been introduced in the chlor-alkali industry and, in 1975, about 50% of the total world production of Cl_2 was achieved with these anodes [1]. Good electrocatalytic properties for O_2 evolution also makes this electrode an interesting material for energy saving in cells for the electrolysis of water.

Electrocatalysis in anodic processes depends on electrode surface preparation and surface morphology as well as the presence and state of surface oxide films on the electrode metal [2]. The surface structure factor in electrocatalysis has also been emphasized by Bagotsky *et al.* [3]. Practically (see below), the real/apparent area ratio is normally of major importance. Low oxygen and chlorine overvoltage is a common characteristic of electrodes based on Ru or RuO_2 [4–14].

The main factors which characterize a good electrocatalyst, in addition to its chemical stability and relative cheapness, are: (a) a high exchange current density, i_0, based on real electrode area; (b) a low Tafel slope, b, so that relatively low overpotentials persist to high current densities. However, the existence of a low Tafel slope process implies that some other process with higher i_0 and b values is prevented from being rate controlling because the subsequent step has a lower rate constant. Practical optimization of electrocatalysis usually aims to minimize polarization by use of high-area electrode materials. Hence it is important, as will be shown in the present paper, to distinguish improved electrocatalytic performance which arises from an increase in the real/apparent area factor from more fundamentally important effects due to increases in rate constant and/or changes of reaction mechanism. For example, in recent work [2] we have shown that the oxide film

* Based on a report to Hooker Chemicals and Plastics Corp., Research Centre, Niagara Falls, NY, July 1976, on a research project supported by Hooker Research Center at the University of Ottawa, 1974–76.
† Permanent address: Ruder Bošković Institute, Zagreb, Yugoslavia, where part of this work (on O_2 evolution electrocatalysis) was carried out by MV.

0021–891X/82/020193–12$03.20/0

on Pt anodes in aqueous solution has electrocatalytic properties for Cl_2 evolution superior to that of Pt metal itself (studied under completely anhydrous conditions in CF_3COOH where no surface oxidation can occur). Also, the co-adsorption of Cl^- ion is an additional and important factor in electrocatalysis for Cl_2 evolution at Pt anode surfaces [15]. In earlier work on Ru, we showed [16, 17] that an interesting change of properties of the surface oxide film, generated in an anodic linear potential sweep, can be developed by repetitive cycling of the electrode anodically and cathodically between *ca* 0.05 and 1.4 V E_H: the formation and reduction of the surface oxide film at Ru is initially highly irreversible for potentials > 0.8 V but becomes remarkably reversible after many anodic/cathodic cycles between *ca* 0.5 and 1.4 V E_H [16–18]. This phenomenon is connected with incomplete reduction of the oxide film in the H adsorption/absorption [19] region and thickening of the film, as at Ir electrodes [20–26]. The reversible behaviour of the oxidation/reduction cycles at such films is no longer connected with formation of a monolayer oxide film and its reduction to the metal (with H adsorbed or sorbed) but with oxidation/reduction redox steps involving several valencies of Ru in a developed oxide film [16–18] thicker than a monolayer. Analogous behaviour has recently been reported for Rh [27] and was also found [16, 17] with a film of RuO_2, thermally formed on glass from $(NH_4)_3RuCl_6$.

In the present paper, we demonstrate that substantial changes of electrocatalytic properties of oxidized Ru surfaces for both the Cl_2 and O_2 evolution reactions arise when Ru electrodes are subjected to a potentiodynamic anodic/cathodic cycling regime of the kind that changes the reversibility of the surface oxide formation and reduction processes. In the present work, however, experiments are restricted to conditions where only a changed state of the 'monolayer' oxide is involved, so that ambiguities concerning changes of real area which can arise at thick, porous oxide films [20–26, 29] are avoided.

2. Experimental procedure

Ruthenized Pt and ruthenized Ru electrodes were prepared by electroplating Ru onto Pt and Ru rod substrate metals. The plating was carried out by application of a cathodic current of 100 μA using a 1 g l^{-1} solution of $(NH_4)_3RuCl_6$ in 0.1 mol dm^{-3} HCl, as described previously [16, 17, 30]. The plated electrodes were then thoroughly washed in multiple changes of pyrodistilled water and finally allowed to stand for 24 h in 1 N H_2SO_4.

The quantity of Ru plated corresponded (cf. [16, 17] to *ca* 5 x 10^3 layers. The deposit of Ru appears, however, to be rough, as in platinization. Some electrodes were plated at 298 K and some at 343 K. Bulk Ru rod electrodes, sealed in glass, were also used.

Potentiodynamic sweeps were made by means of a Wenking potentiostat or a Princeton Applied Research (PAR) Model 174 polarographic analyser and recorded on a Hewlett-Packard Model 7004B *X–Y* recorder. Steady-state potentiostatic polarization measurements were taken after 2 min of polarization at each potential value using the Wenking or PAR Model 173 potentiostat/galvanostat. A Keithley Model 161 digital multimeter was used for potential readings.

Conditioning of the oxidized Ru electrodes by potentiodynamic anodic/cathodic cycling was achieved, as mentioned above, by applying a repetitive sweep up to 1.3–1.4 V E_H in most experiments for 10 to 20 cycles. A changed 'monolayer' state of the oxide film is achieved by limiting the positive end potential in the anodic sweeps to *ca* 1.30 V E_H. If the cycling is taken beyond *ca* 1.4 V E_H into O_2 evolution, then progressive growth of a thick RuO_2 film occurs [16, 17].

A three-compartment electrochemical cell was used. Pt/H_2 or Ag/AgCl reference electrodes were used, depending on the type of experiment. A Ru rod was used as a counter electrode. Electrode potentials are referred to that of the hydrogen electrode in the same solution and designated as E_H V.

In the part of the work carried out at Ottawa,* BDH Aristar grade sulphuric acid was used for the surface oxide formation and reduction studies. Pyrodistilled water [31] was used to make up all solutions. General high purity techniques, including purification of N_2 and H_2, were employed as

* Work on the Cl_2 electrocatalysis at Ru was carried out at the University of Ottawa and extended to O_2 evolution kinetics at Ruder Bošković Institute, Zagreb.

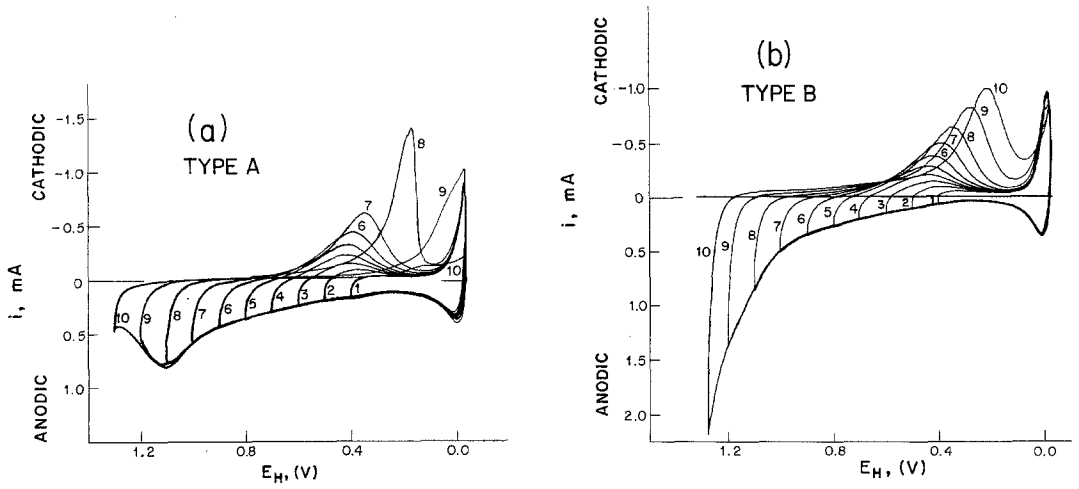

Fig. 1. (a) Potentiodynamic profiles for a ruthenized Pt electrode in 0.5 mol dm^{-3} H_2SO_4 at 16 mV s^{-1} in an N_2-stirred solution at 298 K recorded from − 0.03 V successively to various anodic potentials in 0.1 V increments (Type A surface). (b) Potentiodynamic profile for a ruthenized Pt electrode after 20 cycles from − 0.03 to + 1.1 V at 298 K (Type B electrode). Experimental conditions as in Fig. 1a.

described in previous papers [31, 32]. ACS grade NaCl used in the Cl_2 evolution work was twice recrystallized from solutions in the pyrodistilled water.

In the part of the work conducted in Zagreb, analytical grade sulphuric acid ('Merck', Darmstadt), and sodium chloride ('Kemika', Zagreb), was used. Extra pure nitrogen passed over a heated copper catalyst type BTS, (BASF, Ludwigshafen), was used for solution deaeration. Oxygen was cleaned over heated copper scrapings. Quadruple-distilled water, the last two stages being from a quartz still, was used throughout.

All experiments were carried out at 298 ± 0.2 K.

3. Results

3.1. *Formation of monolayer surface oxide and its reduction at Ru electrodes*

A series of 10 potentiodynamic current versus potential profiles for a ruthenized Pt electrode in 1 N H_2SO_4, taken successively from 0.4 to 1.3 V E_H, are shown in Fig. 1a. The behaviour of a Ru rod electrode is similar [16, 17, 30]. In order to obtain superimposable anodic currents, the potential was held at − 0.3 V for 1 min before each subsequent cycle was started in order to reduce the oxide formed in previous anodic scans. Current versus time experiments [18, 27, 30] have shown that the oxide formed at the most anodic potentials can be reduced within this time period. The true surface area of Ru electrodes cannot be determined as with Pt, using the charge for hydrogen monolayer ionization and deposition, because of the overlap between the H ionization region and the initial surface oxidation processes, and because the H region at Ru corresponds to both absorption and adsorption of H [19, 34, 35]. The currents, therefore, cannot be quantitatively expressed as true current densities.

A freshly prepared electrode, exhibiting the potentiodynamic profile shown in Fig. 1a will be referred to as a Type A electrode in the text which follows.

When the electrode potential is cycled between − 0.03 and + 1.3 V, the form of the potentiodynamic current versus potential profile progressively changes, as shown in Fig. 2 for a succession of 15 cycles. After 15–20 cycles, there are increases of anodic currents between + 0.8 and + 1.3 V, accompanied by shifts of the corresponding surface oxide reduction peak to more positive values. This effect is already established in cycling to 1.1 V E_H in a series of eight successive cycles, as shown in Fig. 3. There is a clear change of state of the oxide film with regard to the reduction peak potential and the half-width and symmetry

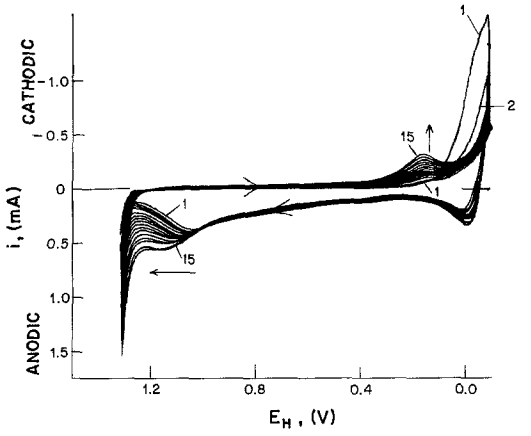

Fig. 2. Effects of cycling a ruthenized Pt electrode at 298 K from − 0.07 to + 1.1 V at 16 mV s^{-1} sweep rate in 0.5 mol dm^{-3} H_2SO_4 showing the progressive change of current versus potential profile over 15 cycles, especially at the anodic end, 1.0–1.3 V E_H.

of the current versus potential profile. The charges under the peaks remain constant within 3%.

The effect of electrode cycling on the complete potentiodynamic profile taken to 1.3 V and lower potentials, as in Fig. 1a, is illustrated in Fig. 1b. An electrode exhibiting this kind of voltammetric behaviour is referred to as a Type B electrode in the text which follows. This type of surface is generated after about 20 cycles and corresponds still to almost a monolayer of RuO_2 species. Thick films can, however, be formed after much more extensive cycling to potentials > 1.4 V and then show the characteristic, very reversible, solid-state redox cyclic–voltammetry profile reported in

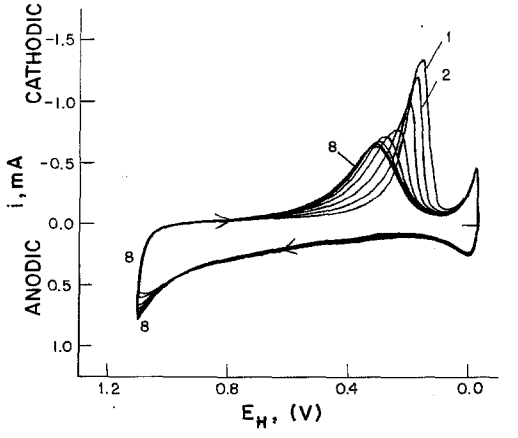

Fig. 3. Change of state of oxidized Ru surface (ruthenized Pt) over eight cycles with cycling to 1.1 V E_H at 298 K as revealed by changes of the cathodic oxide–reduction profile. Sweep rate 16 mV s^{-1}, 0.5 mol dm^{-3} H_2SO_4.

[16, 17]. The latter behaviour is analogous to that known at Ir electrodes [23–26, 29].

In order to establish that the change of behaviour of the oxidized Ru surface upon cycling had nothing to do with the use of Pt as the substrate metal in the case of the ruthenized Pt electrodes (Fig. 1a and b), similar experiments were performed on a ruthenized Ru rod electrode with the results shown in Fig. 4a and b. Evidently such electrodes initially have similar behaviour and also become conditioned by cycling in exactly the same way as those for which Ru was plated on Pt as substrate metal.

Further investigations were made to see whether Type B oxidized Ru surfaces could be generated by *holding* the potential at various anodic limits rather than by cycling. Fig. 5 shows a series of current–potential profiles obtained after holding the potential at 0.8, 0.9 or 1.0 V for 5 min, or at 1.1 V for 40 min, respectively. It is found that these holding times did *not* give rise to any significant change in the potentiodynamic profile: a Type A electrode surface remained (Fig. 5). It is evident, therefore, that the changed oxidized Ru surface can only be generated by successively forming and reducing the oxide layer and therefore allowing the opportunity for some reconstruction of the surface and its oxide to occur. In the presence of Cl^- ion (as NaCl), it is found that this reconstruction occurs much more readily. However, once the reconstructed surface of Type B has been established, it is not possible to regain properties corresponding to the Type A material without physical removal of the Type B film.

While no oxide film changes occur under conditions of potential holding at the above potentials, it is to be noted that major changes in the state and thickness of oxide films at Ru can be made to occur by potential holding at > 1.4 V E_H or by potential cycling to such potentials.

The influence of chloride ions on the potentiodynamic current versus potential profile of the ruthenium electrode was investigated. The behaviour in 5 mol dm^{-3} NaCl is shown in Figs. 6–8. The potentiodynamic profile in 5 mol dm^{-3} NaCl + 0.1 mol dm^{-3} HCl solution (Fig. 6) was recorded using the same experimental procedure as in sulphuric acid alone. The progressive effect of cycling at 20 mV s^{-1} sweep rate is shown in Fig. 7, (cf. Fig. 2). As in the experiments in

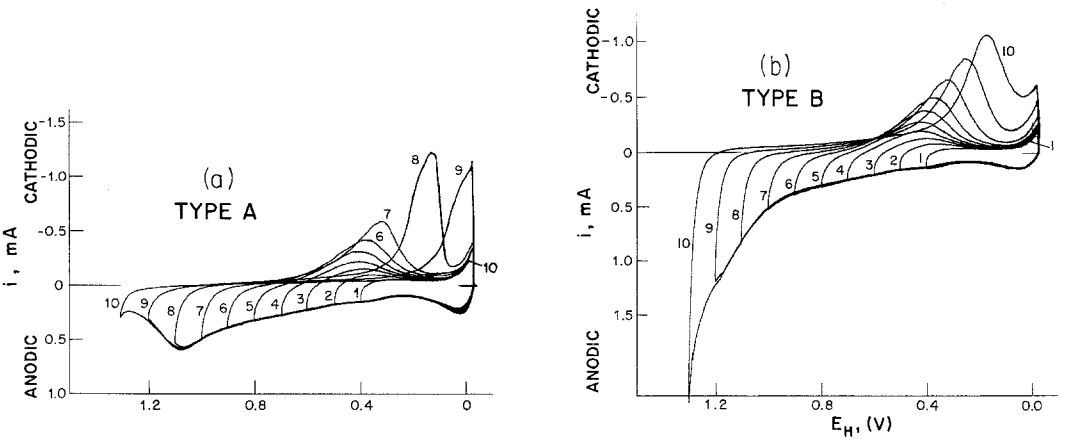

Fig. 4. (a) Initial anodic and cathodic sweep behaviour on a ruthenized Ru rod (cf. Fig. 1a for ruthenized Pt) (conditions as for Fig. 1a). (b) Development of Type B behaviour at a ruthenized Ru rod after cycling to 1.3 V E_H (20 cycles) (conditions as for Fig. 1b).

1 mol dm^{-3} H_2SO_4, the anodic current at + 1.2 V and the corresponding oxide reduction currents increase with cycling, and the anodic peak is shifted to more positive potentials resulting finally in a current–potential profile typically presented in Fig. 8 and having Type B characteristics. This Type B electrode, when transferred to 1 mol dm^{-3} H_2SO_4 solution showed the same profile as that in Fig. 1b, i.e. after cycling in sulphuric acid alone. Visual observation of the electrodes showed that the colour of a freshly prepared Type A electrode had become changed from bright grey to almost black by the time Type B electrode behaviour had developed, yet the real area, as measured by the oxide reduction charge on the cathodic sweep, had changed by < 5%.

The anodic currents in the H region during cycling (Fig. 8), as in H_2SO_4, are also smaller in each successive cycle due to some dissolution of Ru. This process is indicated in chloride solution by the eventual appearance of a pale yellow colour in the electrolyte during prolonged cycling or after many experiments.

In the presence of Cl^- ion (5.1 mol dm^{-3}), it is seen that the initial stage of surface oxidation of Ru becomes better separated from the region of anodic currents for adsorbed and absorbed [19] H ionization. This is due to the familiar effects of

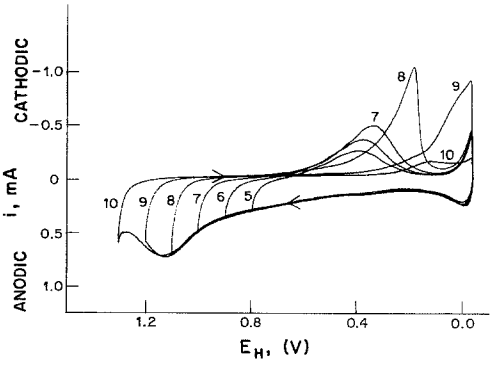

Fig. 5. Effects of holding the potential at various values (0.8, 0.9, 1.0 V E_H) on a ruthenized Ru electrode for 5 min or at 1.1 V for 40 min in the subsequent oxidation/reduction behaviour. The sweeps shown are taken after the holding periods; Type A surface remains.

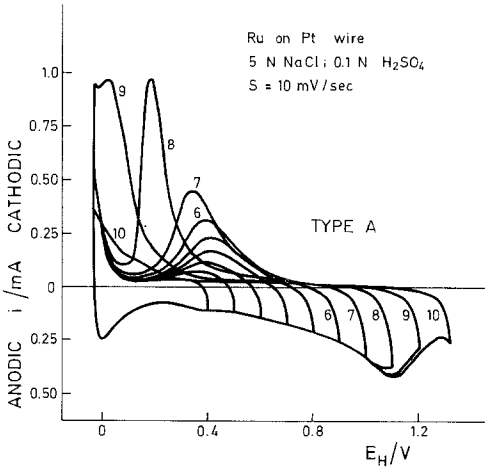

Fig. 6. Potentiodynamic i versus V profiles for ruthenized Pt taken to successively increasing positive potentials in 5 mol dm^{-3} NaCl + 0.1 N H_2SO_4 (298 K). Sweep rate 10 mV s^{-1} (Type A behaviour). (Figs. 6, 7 and 8 were recorded with opposite x-axis polarity to that in the other cyclic-voltammetry curves).

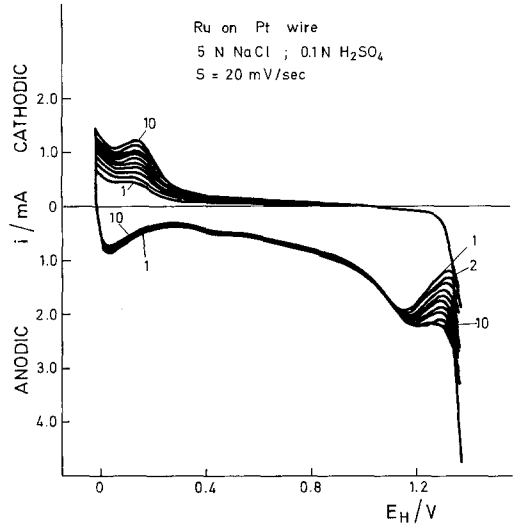

Fig. 7. Progressive change of state of oxidized Ru surface (at ruthenized Pt) with cycling at 20 mV s^{-1} as revealed by changes of the cathodic oxide reduction i versus V profile and the currents at the positive end of the sweep. 5 mol dm^{-3} NaCl + 0.1 mol dm^{-3} H_2SO_4 (298 K).

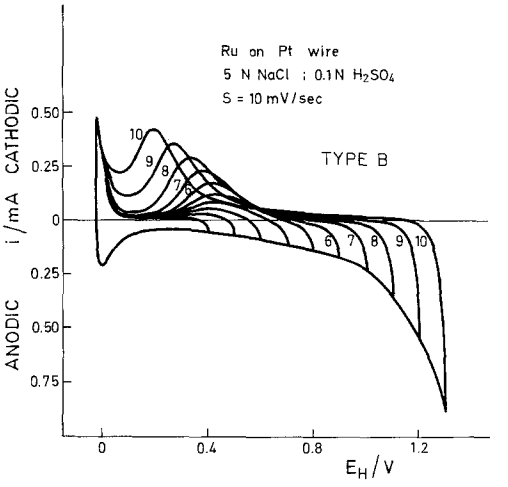

Fig. 8. As in Fig. 6 but after 10 anodic/cathodic cycles in 5 mol dm^{-3} NaCl + 0.1 mol dm^{-3} H_2SO_4 (298 K). Type B behaviour is generated.

strongly adsorbed anions in displacing initial stages of surface oxidation to more positive potentials and the H region to less positive potentials due to competitive adsorption [36, 37]. If the oxide film is thickened beyond 2 monolayers (cf. [16, 17]), these effects of Cl^- adsorption are not observed because the metal remains covered with oxide over the whole potential range of *ca* 0.0–1.3 V.

3.2. *Effects of plating ruthenium at elevated temperature*

Some studies were made on the effects of electrodeposition of Ru at a Pt substrate at elevated temperatures, rather than at room temperature. It is found that an increase in plating temperature gives better current efficiencies for ruthenium deposition (i.e. less co-evolution of hydrogen) and a more coherent and brighter deposit of Ru results. Fig. 9a shows the potentiodynamic current versus potential profiles for a ruthenized Pt electrode plated at 343 K but recorded at 298 K. The appearance of the main peak around 1.0 V is similar to that of Type A electrodes prepared by plating at 298 K and the corresponding series of reduction profiles is also similar. However, for the electrode plated at 343 K, there is an enhanced peak at 0.3 V where the initial stage of oxidation commences. This is not observed so clearly on electrodes plated at the lower temperature. Fig. 9b shows a series of successive sweep profiles from the H region to the Cl_2 evolution region where the progressive change of the surface is evident. However, the effects are rather less than those observed on the 298 K plated material, illustrated in Fig. 1a and b. A characteristic property of this

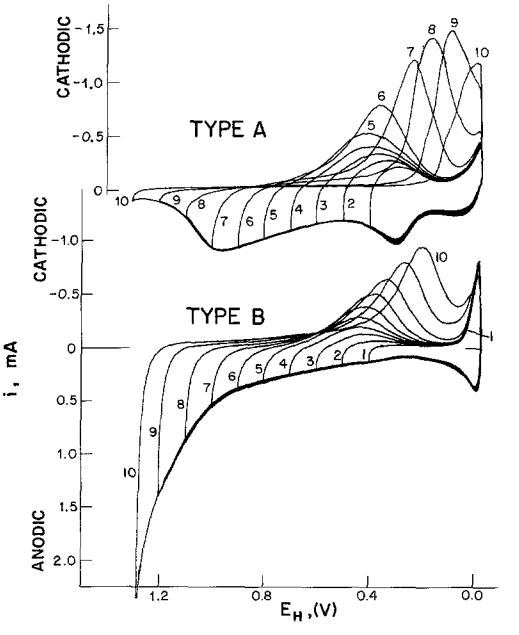

Fig. 9. Change from Type A to Type B surface at a ruthenized Pt surface plated at 343 K (conditions otherwise as for Fig. 1a).

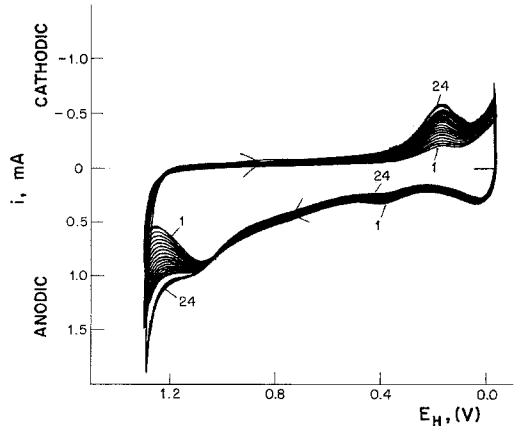

Fig. 10. Succession of 24 current versus potential profiles for potentiodynamic cycling of a ruthenized Pt electrode plated at 343 K in 0.5 mol dm^{-3} H_2SO_4. (Compare Fig. 2; conditions otherwise as for Fig. 1a.)

type of electrode is that it takes a much longer cycling time for the Type B state of the surface to be attained. Progress towards the Type B condition is illustrated in the series of profiles shown in Fig. 10 over 24 cycles.

3.3. *Kinetics of electrochemical chlorine evolution on Type A and Type B oxidized surfaces of Ru*

Current–potential relations for Cl_2 evolution were measured, point-by-point, over the range of current 0.01 to 100 mA. Tafel relations for ascending and descending changes of potential were made successively over this range of current. Real current–densities are not specified owing to the uncertain real area of the electrode preparations mentioned earlier. All experiments were carried out in 5 mol dm^{-3} NaCl solutions at 25° C. Fig. 11 shows a series of *IR* corrected log(current) versus potential relations for Cl_2 evolution on ruthenized Pt electrodes for the first run at increasing and decreasing currents on Type A electrodes and for runs with increasing and decreasing currents on Type B electrodes, that is, for ascending or descending changes of controlled potential.

It is seen from Fig. 11 that very substantial increases in Cl_2 evolution rates are achieved in going from the initial stage (Type A) of oxidation of the surface through some intermediate states where some runs at ascending and descending potentials were carried out, to the final state of the electrode when it is of Type B character. At an overpotential of *ca* 0.05 V, the Cl_2 evolution current increases by a factor of 30.

For electrodes ruthenized at 343 K, a smaller current increase, by a factor of 5, results from conditioning by anodic/cathodic cycling, but again no significant area change is involved, as indicated by the more or less constant current values in the hydrogen region and the initial surface oxidation region.

It appears that Ru surfaces plated at elevated temperatures are more stable than those prepared at lower temperatures. This may be expected thermodynamically.

Both types of electrode, prepared under either of the conditions of plating give rather similar curved log(current) versus potential relations but not of the kind (cf. [2]) that correspond to re-

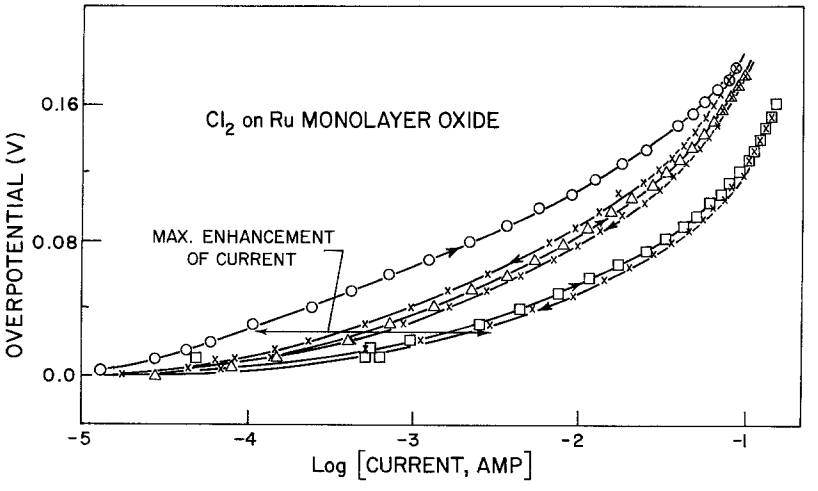

Fig. 11. Enhancement of anodic Cl_2 evolution currents after progressive cycling of a ruthenized Pt electrode (conditions as for Fig. 1). Tafel relations measured at 298 K. First run, increasing anodic potentials ○; first run, decreasing anodic potentials X; Fifth run, increasing anodic potentials △; fifth run, decreasing anodic potentials X. After formation of Type B surface: Increasing anodic potentials □; decreasing anodic potentials X.

combination (of Cl^-) control. The mechanism of Cl_2 evolution at oxidized Ru does not therefore appear to be changed by the cycling treatment and may correspond to the pathway proposed by Krishtalik and Erenburg [38].

In considering the significance of this enhancement of Cl_2 evolution current in going from a Type A state of the surface to a Type B one, an important question is whether the real area of the electrode has increased appreciably. Inspection of Fig. 1a and b show that the current–potential profiles for the H oxidation region and for the following initial stages of surface oxidation of the Ru are hardly changed by the cycling regime. It is evident, therefore, that the observed substantial increases (30 x) of Cl_2 evolution currents on Type B electrode surfaces in comparison with Type A ones occur on Ru surfaces that have *not changed in area by more than ca 5%.* A true increase of electrocatalytic effectiveness of the surface for anodic Cl_2 evolution has therefore been generated by the electrode cycling treatment.

3.4. *Kinetics of electrochemical oxygen evolution on Type A and Type B oxidized surfaces of Ru*

The electrode kinetics of O_2 evolution were also investigated on Type A and Type B Ru electrodes. Fig. 12 shows the potentiostatic steady-state current versus potential relations in 0.5 mol dm^{-3} H_2SO_4 at 298 K. Both types of electrode surface give 30 mV/decade Tafel slopes with about eight times higher currents at the same potential for Type B electrodes in comparison with Type A electrodes in the linear Tafel region. Above + 1.5 V a sharp decrease in current occurs at both electrodes due either to ruthenium dissolution or to passivation by a new state of the surface (cf. [40]). A voltammogram recorded after the polarization measurements at this high potential showed considerably lower currents over the whole voltage range indicating the former effect as the likely reason for the decrease of O_2 evolution currents.

The similarity of shapes of the log(current) versus potential relations for O_2 evolution shown in Fig. 12 indicates that the mechanism of O_2 evolution is not changed in going from the Type A to the Type B surface. A similar conclusion was reached above for Cl_2 evolution kinetics.

4. Discussion

Comparison of Fig. 1a and b shows that changes in the potentiodynamic current–potential profile for a ruthenized electrode occur when it is subjected to repetitive cycling from + 0.06 to + 1.1 V. The anodic peak at + 1.1 V shifts to more positive potentials, merging finally into the region of the O_2 or Cl_2 evolution reactions. Relatively slow sweep rates have been used in these potentiodynamic experiments, as it is usually found (cf. [19] and [30]) that a slow sweep, taken to successively more positive potentials, can better resolve the several overlapping surface oxidation–reduction processes at a Ru electrode. Other regions of the i–V profile (Fig. 2) are somewhat

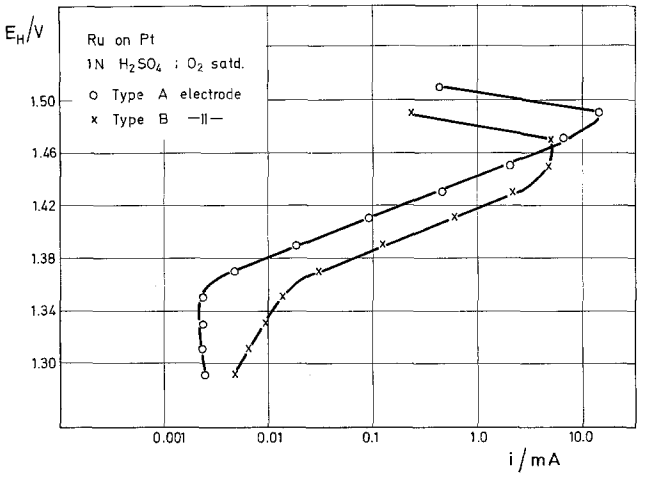

Fig. 12. Potentiostatic current versus potential relations for O_2 evolution on ruthenized Pt (plated at 298 K) in Type A and Type B states.

influenced by repetitive cycling but only in the direction of decreasing anodic current over the H ionization region from + 0.06 to + 0.3 V and over the initial oxide formation region up to + 0.8 V. Potential cycling conditioning, therefore, does not produce a rougher surface. If anything, the surface area becomes a little smaller due to Ru dissolution, as may be detected in acidic [7, 8, 10] or in chloride solutions [4, 16, 17]. In the present experiments, development of a yellow colour in chloride solutions indicated ruthenium dissolution after prolonged cycling.

According to Llopis *et al.* [4] the dissolved species are $RuCl_6^{3-}$ or $RuCl_6^{2-}$, depending on potential.

Chloride ions are strongly adsorbed at platinum and it was shown by Breiter [36] that at 10^{-2} mol dm^{-3} concentration they almost completely inhibit Pt surface oxidation. However, such effects are much smaller on ruthenium [4, 19, 41] although the present results show (cf. [37]) that the initial stage of surface oxidation of ruthenium is displaced to more positive and hydrogen adsorption to more negative potentials, as also found at Pt.

The Type B electrode surface is also formed in the presence of chloride ions during repetitive cycling, but less irreversible surface oxidation–reduction processes are then observed (Fig. 8). When this electrode is transfered to sulphuric acid, the same i–V profile as observed for the electrode cycled in sulphuric acid is found. This indicates that the same surface reconstruction processes are involved during potential cycling in H_2SO_4 or Cl^- solutions, giving rise to Type B electrode formation. The differences when Cl^- ions are present are therefore due only to Cl^- ion adsorption.

The most interesting property of the Type B electrode surface is its better electrocatalytic behaviour for the Cl_2 and O_2 evolution reactions, an effect which is not due to area changes.

For O_2 evolution, both types of electrode give 30 mV/decade Tafel slopes indicating that the mechanism of oxygen evolution remains the same for both surfaces. The same Tafel slope for O_2 evolution on Ru has been observed by Iwakura *et al.* [10] and the mechanism proposed by those authors is the recombination of two adsorbed hydroxyl intermediates as the rate determining step.

That Type B electrode surfaces give better electrocatalytic effectiveness can be explained on the basis of the discussion given by Tseung and Jasem [42] who pointed out the role of the metal/metal oxide or lower valent metal oxide/higher valent metal oxide couples in the O_2 evolution reaction on semiconducting oxides. According to those authors, a good electrocatalyst will be one whose redox couple is close to, or at, the potential of the O_2 electrode in the same medium.

The anodic peak observed in the surface oxidation of a Ru electrode at + 1.1 V (Fig. 1a) can be ascribed to development of the Ru(III)/Ru(IV) couple [18, 19, 43]. Its shift towards positive values during repetitive cycling provides conditions at the electrode surface which are more favourable for Cl_2 or O_2 evolution, giving rise to the observed increase in Cl_2 or O_2 evolution rates at the Type B electrode by almost an order of magnitude (Figs. 11 and 12).

Since this work was completed (see footnote on title page), it has been found that some other noble metals exhibit enhanced O_2 evolution rates after conditioning by potential cycling: Burke and O'Sullivan [27] observed an increase of oxygen evolution current and a lower Tafel slope when a rhodium electrode was subjected to potential cycling in alkaline solution, and a similar activation of iridium electrodes for O_2 evolution from aqueous H_2SO_4 solution was reported by Gottesfeld and Srinivasan [22]. They explained the improved electrode activity for O_2 evolution by a change in the stoichiometry of the oxide film corresponding to an increased oxidation state of the metal. This is probably also the case with oxidized Ru where, in successive cycles, the exchange of protons in cycling between Ru(III) and Ru(IV) oxides takes place [16–18], increasing the average oxidation state of Ru in the surface oxide film in every subsequent cycle, creating more favourable conditions for adsorption of $OH^{\cdot}$ or $Cl^{\cdot}$ intermediates and their subsequent reactions to form O_2 or Cl_2.

Since the mechanisms of O_2 and Cl_2 evolution are usually different on most metals, the electrocatalytic effect observed here appears to be of a general type connected with the oxidation state and probably the electronic structure of the catalytic monolayer oxide films.

It is unlikely that a surface cleaning effect [31] is the reason for the effects described above, as might arise at Pt. In that case adsorbed impurities

result [31, 44, 45] in (a) blocking of hydrogen ionization and adsorption processes; (b) blocking the initial region of surface oxidation and (c) an increase of current in the far anodic region where oxidation of adsorbed impurities takes place at Pt. In the presence of impurities, cycling reverses these effects. They are, however, not observed during potential cycling of ruthenized electrodes. Thus, after 2–3 cleaning cycles in the present experiments, anodic currents tend to increase in the far anodic region while an increase of H ionization current is not observed, indicating that it is the changes in the stoichiometry of the oxide film, discussed above, that contribute predominantly to the change in the potentiodynamic profiles and not removal of impurities.

It appears that the presence and oxidation state of an oxide film on an anode is a critical factor in the kinetics of various continuous oxidation processes that can take place on such a surface. This is already indicated by the critical state of Pt surface oxidation required for occurrence of the Kolbe reaction with any reasonable efficiency [46], and the required presence of some surface oxide at Pt for favourable Cl_2 evolution rates [2]. It is also indicated from Burshtein's observation [47] that a critical state of surface oxidation of Au electrodes is required for the onset of O_2 evolution at that metal and our own observation [37] that adsorbed anions (CO_3^{2-}, $B_4O_7^{2-}$) have a strong influence on that critical condition.

From the current–potential profiles of Fig. 1a and b for Ru, it is evident that anodic/cathodic cycling primarily shifts to more positive values the potential range over which the higher state of oxidation in the surface oxide film develops and a corresponding electrochemical stability of this state arises as measured by the potential range of the corresponding reduction peak on the cathodic profile (Fig. 1a and b). If this stage of oxidation in the oxide film is critically required as a good catalytic mediator for a step in the Cl_2 and O_2 evolution reactions, these will tend to be facilitated. It appears that for the uncycled oxide film, the peak for the higher oxidation state (0.8 to 1.28 V E_H) is completed at 1.28 V. In the cycled electrode, this oxidation state is shifted to more positive potentials so the peak for this process is incomplete at potentials where significant rates of O_2 and Cl_2 can arise.

Neither the O_2 nor the Cl_2 evolution processes have any of the characteristics of electrode kinetics modified by resistive effects in a film, so that the change of kinetics must be attributed to (a) changes of adsorption conditions for intermediates in the reaction or for adsorption of the Cl^- ion [15] in the case of Cl_2 evolution or (b) changes in electron transfer rate constants. The provision of mixed Ru(III)/Ru(IV) valency states [16, 17] rather than a complete Ru(IV) state in the oxide film at the surface of the cycled Ru electrode could provide more facile anodic electron transfer due to electron vacancies corresponding to Ru(III) states. At the moment, the origin of these substantial electrocatalytic effects must remain speculative but they are, we believe, of considerable practical and theoretical interest.

In the case of activation effects at Ir and Rh electrodes for O_2 evolution described in papers published [25, 27–29, 40] since this work was completed, quite thick films are generated by the cycling regime and their structure and morphology can be seen easily in scanning electron microscope photographs [49]. In these cases, it is possible that the kinetically significant real area has changed although the double-layer capacitance and H accommodation, e.g. at cycled Ir electrodes bearing microscopically visible oxide films, is surprisingly, unchanged. This effect is now understood [49] in terms of a 'conductivity switched' change of activity of the electrode due to the large area of the developed, thick porous oxide film being unavailable for H or double-layer charging because of a potential-dependent conductivity decrease below 0.6 V E_H (at Ir).

In the present case, with Ru, the extent of cycling was limited so that thick films, which otherwise also grow on Ru as at Ir, were not formed. In fact, the cyclic voltammograms in Figs. 3 and 4 for Ru after cycling, correspond to formation and reduction of quantities of surface oxide that hardly differ from that in the initial anodic/cathodic sweeps (Figs. 1 and 4). When thicker oxide films are formed (as in the case of Ir), the cyclic voltammogram shows remarkably reversible behaviour over the whole potential range from 0.05 to 1.4 V E_H, as we showed in [16, 17].

It is interesting that if thick films of oxide are developed at Ru by anodic/cathodic cycling and Cl_2 is evolved upon them, Cl_2 evolution rates are

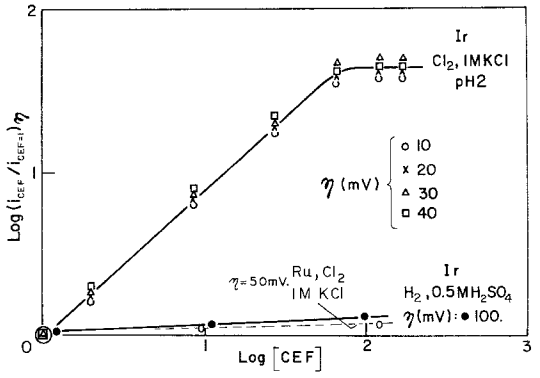

Fig. 13. Comparison of enhancement of anodic Cl_2 evolution rates at 298 K from 1.0 mol dm^{-3} KCl + 0.01 mol dm^{-3} HCl on thick film oxidized Ir electrodes and on thick film oxidized Ru electrodes in terms of film thickness as measured by the charge enhancement factor CEF. Also shown is the H_2 evolution behaviour at oxidized Ir surfaces where, at cathodic potentials, the thick oxide film is relatively non-conducting (contrast Ru where the thick film is conducting).

hardly enhanced at all in contrast to the substantial (180 times) increase observed at Ir [49] (Fig. 13).

Acknowledgments

Grateful acknowledgment is made to Hooker Research for support of this work and provision of a Research Fellowship to MV. The interest of Drs D. Pouli and D. Stevens (at Hooker Research), and Dr V. Pravdić at Ruder Bosković Institute, in this research has been much appreciated. Complementary support from National Research Council grant funds, which provided a Senior Research Fellowship to one of us (HAK), is also gratefully acknowledged.

References

[1] K. Haas and P. Schmittinger, *Electrochim. Acta* **21** 115 (1976).
[2] B. E. Conway and D. M. Novak, *J. Electroanal. Chem.* **99** (1979) 133.
[3] V. S. Bagotzky, Y. B. Vassilyev and I. Pyshnograeva, *Electrochim. Acta* **16** (1971) 2141.
[4] J. Llopis, I. M. Tordesillas and J. M. Alfayate, *ibid.* **11** (1966) 623.
[5] S. Trasatti and G. Buzzanca, *J. Electroanal. Chem.* **29** (1971) App. 1.
[6] D. Galizzioli, F. Tantardini and S. Trasatti, *J. Appl. Electrochem.* **4** (1974) 57.
[7] I. E. Veselovskaya, S. D. Khodkevich, R. I. Malkina and L. M. Yakimenko, *Elektrokhimiya* **10** (1974) 74.
[8] L. D. Burke and T. O. O'Meara, *J. Chem. Soc. Faraday Trans. I* **68** (1972) 839.
[9] W. O'Grady, C. Iwakura, J. Huang and E. Yeager, in 'Electrocatalysis', (edited by M. W. Breiter), The Electrochemical Society Symposium Series, Princeton, NJ (1974) p. 286.
[10] C. Iwakura, K. Hirao and H. Tamura, *Electrochim. Acta* **22** (1977) 329.
[11] *Idem, ibid.* **22** (1977) 335.
[12] G. Lodi, E. Sivieri, A. de Battisti and S. Trasatti, *J. Appl. Electrochem.* **8** (1978) 135.
[13] L. D. Burke, O. J. Murphy, J. F. O'Neill and S. Venkatesan, *J. Chem. Soc. Faraday Trans. I* **73** (1977) 1659.
[14] M. H. Miles, E. A. Klaus, P. B. Gunn, J. R. Locker, W. E. Serafin and S. Srinivasan, *Electrochim. Acta* **23** (1978) 521.
[15] B. E. Conway and D. M. Novak, *J. Chem. Soc. Faraday Trans. I* **75** (1979) 2454.
[16] S. Hadži-Jordanov, H. Angerstein-Kozkowska, M. Vuković and B. E. Conway, *J. Electrochem. Soc.* **125** (1978) 1471.
[17] *Idem, Electrochemical Society Symposium on Electrode Materials and Processes for Energy Conversion and Storage,* (edited by J. D. McIntyre, S. Srinivasan and F. G. Will), The Electrochemical Society, Vol. 77–6, (1977) p. 185.
[18] D. Michell, D. A. J. Rand and R. Woods, *J. Electroanal. Chem.* **89** (1978) 11.
[19] S. Hadži-Jordanov, H. Angerstein-Kozlowska, M. Vuković and B. E. Conway, *J. Phys. Chem.* **81** (1977) 2271.
[20] D. Michell, D. A. J. Rand and R. Woods, *J. Electroanal. Chem.* **84** (1977) 117 and references therein.
[21] D. N. Buckley and L. D. Burke, *J. Chem. Soc. Faraday Trans. I* **71** (1975) 1447.
[22] S. Gottesfeld and S. Srinivasan, *J. Electroanal. Chem.* **86** (1978) 89.
[23] W. Visscher and M. Bleilevens, *Electrochim. Acta* **19** (1974) 387.
[24] J. M. Otten and W. Visscher, *J. Electroanal. Chem.* **55** (1974) 13.
[25] J. O. Zerbino, N. R. Tacconi and A. J. Arvia, *J. Electrochem. Soc.* **125** (1978) 1266.
[26] A. Capon and R. Parsons, *J. Electroanal. Chem.* **39** (1972) 275.
[27] L. D. Burke and E. J. M. O'Sullivan, *J. Electroanal. Chem.* **93** (1978) 11.
[28] *Idem, ibid.* **97** (1979) 123.
[29] E. J. Fraser and R. Woods, *J. Electroanal. Chem.* **102** (1979) 127.
[30] S. Hadži-Jordanov, H. Angerstein-Kozkowska and B. E. Conway, *ibid.* **60** (1975) 359.
[31] B. E. Conway, W. B. A. Sharp, H. Angerstein-Kozlowska and E. E. Criddle, *Anal. Chem.* **45** (1973) 1331.
[32] E.g. see H. Angerstein-Kozkowska and B. E. Conway, *J. Electroanal. Chem.* **43** (1973) 9.
[33] J. D. Burke and J. K. Mulcahy, *ibid.* **73** (1976) 207.
[34] E. K. Tuseeva, A. M. Skundin and V. S. Bagotzky, *Elektrokhimiya* **9** (1973) 1541.
[35] V. S. Bagotzky, A. M. Skundin and E. K. Tuseeva, *Electrochim. Acta* **21** (1976) 29.

[36] M. W. Breiter, *ibid.* **8** (1963) 925.
[37] B. E. Conway, H. Angerstein-Kozkowska, B. Barnett and J. Mozota, *J. Electroanal. Chem.* **100** (1979) 417.
[38] R. G. Erenburg, L. I. Krishtalik and V. I. Bystrov, *Electrokhimiya* **8** (1972) 1740.
[39] R. G. Erenburg, L. I. Krishtalik and I. P. Yaroshevskaya, *Electrokhimiya* **11** (1975) 1068, 1072.
[40] S. Srinivasan and P. W. T. Yu, *J. Electrochem. Soc.* **125** (1978) 1416.
[41] J. Llopis and M. Vazquez, *Electrochim. Acta* **11** (1966) 633.
[42] A. C. C. Tseung and S. Jasem, *ibid.* **22** (1977) 31.
[43] J. F. Llopis and I. M. Tordesillas, in 'Encyclopedia of Electrochemistry of the Elements', (edited by A. J. Bard) Marcel Dekker, New York (1966) p. 277.
[44] S. Gilman, in 'Electroanalytical Chemistry', (edited by A. J. Bard) Marcel Dekker, New York, Vol. 2 (1967) p. 111.
[45] R. Woods, in 'Electroanalytical Chemistry', (edited by A. J. Bard) Marcel Dekker, New York, Vol. 9 (1976) p. 1.
[46] E.g. see A. K. Vijk and B. E. Conway, *Chem. Rev.* **67** (1967) 623.
[47] R. K. Burshtein, *Elektrokhimiya* **3** (1967) 349.
[48] *Idem, ibid.* **6** (1970) 1497.
[49] B. E. Conway and J. Mozota, *J. Electrochem. Soc.* **128** (1981) 2142.